ԵՐԵՎԱՆԻ ՖԻԶԻԿԱՅԻ ԻՆՍՏԻՏՈՒՏ
ЕРЕВАНСКИЙ ФИЗИЧЕСКИЙ ИНСТИТУТ

ЕФИ-464(6)-81

G.G.ARAKELIAN, A.A.GRIGORYAN

INCLUSIVE SPECTRA OF Δ^{++} -ISOBAR IN HADRON-HADRON COLLISIONS

ԵՐԵՎԱՆ 1981 ЕРЕВАН

YEREVAN PHYSICS INSTITUTE

G.G.ARAKELIAN, A.A.GRIGORYAN

INCLUSIVE SPECTRA OF Δ^{++} -ISOBAR IN HADRON-HADRON COLLISIONS

Yere[illegible] 1981

ЕФИ-464(6)-81

G.G.ARAKELIAN, A.A.GRIGORYAN

INCLUSIVE SPECTRA OF Δ^{++}-ISOBAR IN HADRON-HADRON COLLISIONS

The comparison of experimental data on Δ^{++}-isobar inclusive spectra in πP, PP and $\bar{P}P$-collisions with the predictions of reggeised π-meson exchange model OPER is carried out. The model describes quantitatively the majority of experimental data. The question of $\pi^{0}N$, $\pi\pi$, $K\pi$ and $\gamma\pi$ total cross section extraction from the data on the inclusive spectra of Δ-isobar is discussed.

Yerevan Physics Institute

Yerevan 1981

ЕФИ-464(6)-81

Г.Г.АРАКЕЛЯН, А.А.ГРИГОРЯН

ИНКЛЮЗИВНЫЕ СПЕКТРЫ Δ^{++} -ИЗОБАРЫ В АДРОН-АДРОННЫХ СТОЛКНОВЕНИЯХ

Проводится анализ экспериментальных данных по спектрам Δ^{++} -изобары в πp , pp и $\bar{p}p$ - столкновениях и сравнение их с предсказаниями модели реджезованного π -мезонного обмена $OPER$. Модель количественно описывает большинство экспериментальных данных. Обсуждается вопрос об извлечении из данных по спектрам Δ -изобары полных сечений $\pi^{*}N$, $\pi\pi$, $K\pi$ - и $\gamma\pi$ - взаимодействий.

Ереванский физический институт
Ереван 1981

1. Introduction

Inclusive spectra of Δ^{++} -isobar in πp - and pp -collisions have been earlier investigated within the framework of reggeised one-pion-exchange model (OPER) [1,2]. It has been shown in these works that with a few parameters the OPER-model successfully describes the characteristics of these spectra in unit parametrization. Recently a lot of new experimental data on Δ^{++}-isobar spectra in hadron-hadron collisions [3-6] appeared and it is interesting to analyse these data in OPER-model.

In this paper the OPER-model predictions are compared with the experimental data on reactions

$$\pi^- p \to \Delta^{++} X \qquad \text{(Ia)}$$

$$\pi^+ p \to \Delta^{++} X \qquad \text{(Ib)}$$

$$p p \to \Delta^{++} X \qquad \text{(Ic)}$$

$$\bar{p} p \to \Delta^{++} X \qquad \text{(Id)}$$

in a large energy interval of 22 ÷ 360 GeV.

In Sec. 2 the model is formulated. In Sec. 3 the theoretical calculations are compared with experimental data. In Sec. 4 the problem of extraction of $\pi^* N$, $\pi\pi$, $K\pi$ and $\gamma\pi$ total cross sections from the data on Δ -isobar spectra is considered.

2. Formulation of the model

In CFIR-model the spectra of Δ^{++} -isobar in ap -scattering ($a = \pi, P, \bar{P}$) in proton fragmentation region are described by a diagram in Fig. 1. The cross section corresponding to this diagram has the form

$$E\frac{d^3\sigma}{d^3p} = \frac{G_\Delta(t)}{4P_0^*\sqrt{S}}|F_\Delta(S,S_1,t)|^2[4P_\pi\sqrt{S_1}\,\sigma_{tot}^{\pi a}(S_1)] \qquad (2)$$

where

$$S = (P_p + P_a)^2;\ S_1 = (P_p + P_a - P_\Delta)^2;\quad t = (P_\Delta - P_p)^2$$

the momenta P_p, P_a and P_Δ are described in Fig. 1, P_0^* is the momentum in ap c.m.s.; P_π is the pion momentum in c.m.s. of virtual π -meson and particle a ; $\sigma_{tot}^{\pi a}$ is the total cross section of i sort on-mass-shell π -meson scattering on particle a. $G_\Delta(t)$ is the vertex function averaged over nucleon spin

$$G_\Delta(t) = g^2_{pn\pi\Delta}\,\frac{[(m_\Delta - m)^2 - t][(m_\Delta + m)^2 - t]^2}{6m_\Delta^2} \qquad (3)$$

$$g^2_{p n \pi^+ \Delta^{++}}/4\pi = 19\ GeV^2$$

The formfactor $F_\Delta(S,S_1,t)$ describing the off-mass-shell corrections has the following form

$$F_\Delta(s,s_1,t) = e^{\Lambda(t-\mu^2)} \times \begin{cases} \dfrac{\alpha'_\pi \pi}{2\sin\left[\frac{\pi}{2}\alpha'_\pi(t-\mu^2)\right]}, & |t| < |t_0| \\ \dfrac{\alpha'_\pi \pi}{2\sin\left[\frac{\pi}{2}\alpha'_\pi(t_0-\mu^2)\right]}\, e^{R_2^2(t-t_0)}, & |t| > |t_0| \end{cases} \qquad (4)$$

$$\Lambda = R_1^2 + \alpha'_\pi \ln\frac{S\,S_0}{S_1\,m_\Delta^2};\quad S_0 = 1\ GeV^2$$

m_Δ, m, μ are the masses of Δ -isobar, nucleon and π -meson, respectively. On the matching point the continuity condition was imposed on the formfactor as well as on its first derivative, connecting the parameter t_0 with R_2^2, and only the parameters R_1^2 and t_0 remain independent. They are found from the comparison with experimental data

$$t_0 = -0.7\,(GeV/c)^2; \quad R_1^2 = 0.6\ GeV^{-2} \qquad (5)$$

and then

$$R_2^2 = 0.74\ GeV^{-2}$$

It should be mentioned, that the values of the parameters (5) somewhat differ from those of the works [1,2], where the continuity condition of the derivative was not imposed. When compared with experimental data, a correction must be taken into account, connected with the experimental cut-off on the mass of π^+p -system. Assuming the Breit-Wigner distribution the formula (2) is multiplied by coefficient $a(\Gamma_\Delta)$

$$a(\Gamma_\Delta) = \frac{1}{\pi}\left(\operatorname{arctg}\frac{m_u^2 - m_\Delta^2}{m_\Delta \Gamma_\Delta} + \operatorname{arctg}\frac{m_\Delta^2 - m_e^2}{m_\Delta \Gamma_\Delta}\right) \qquad (6)$$

where m_u and m_e are the upper and lower limits of the experimental cut-off, Γ_Δ is the Δ -resonance width.

3. Comparison with experimental data

a) Dependence on x and M_x

At high energies the shape of Δ -isobar spectra in the proton fragmentation region is similar to that of nucleon charge-exchange inclusive spectra (they both are described by $\pi\pi P$ triple-Regge diagram and have scaling form).

The comparison of the experimental data on X-dependence of the reactions Ia-d with OPER-model calculations is given in Fig. 2. In Fig. 2a the invariant cross section

$$F(x) = \int \frac{E^*}{\pi P^*_{max}} \quad \frac{d^2\sigma}{dx\, dP_\perp^2}\, dP_\perp^2$$

for the reaction Id at 22.4 GeV/c is presented [6].
In this experiment the Δ^{++}-isobar was determined by π^+p-system mass cut-off in the interval of $1.16 < M < 1.32$ GeV. Here the cut-off $|t| \leq 0.74$ GeV^2 has been imposed. The invariant cross section $F(x) = \int \frac{E}{\pi P_0^*} \frac{d^2\sigma}{dx\, dP_\perp^2}\, dP_\perp^2$ as a function of $x = \frac{P_\parallel^*}{P_0^*}$ for the reaction Ib at momentum 32 GeV/c and $|t| \leq 0.6$(GeV/c)^2 is shown in Fig. 2b ($1.16 < M < 1.32$ GeV).

The behaviour of the cross section $d\sigma/dx$ for the reactions Ia,b,c at 147 GeV/c and $|t| \leq 1$(GeV/c)^2 [4] is given in Fig. 2c-e. Two types of points in Fig. 2c-e (see below Fig. 5c-e and Fig. 7c-e) correspond to two methods of experimental data processing:

a) The distribution on π^+p-system mass was fitted separately for each experimental interval of the variable, using the Breit-Wigner distribution (white circles);

b) the distribution was obtained for the mass interval $1.12 < M < 1.32$ GeV (black circles).

In Fig. 2f the invariant cross section of the reaction Ia

$$F(x) = \int \frac{2E}{\pi\sqrt{s}} \cdot \frac{d^2\sigma}{dx\, dP_\perp^2}\, dP_\perp^2\,; \quad x = 2P_\parallel^*/\sqrt{s}$$

is given at momenta 100, 200, 360 GeV/c [3] and $|t| \leq 1$(GeV/c)^2.
The two scales in Fig. 2f (see also Figs 4b,c, 5f, 6c) correspond to two parametrizations of background under Δ^{++}-isobar:

a) The left scale corresponds to the parametrization of background in quadratic polynomial; b) the right scale - in cubic polynomial. Theoretical curves in Fig. 2f are calculated at 360 GeV/c. The lower curve in Fig. 2f (in Figs 4b,c, 5f 6c as well) corresponds to the left scale, the upper curve - to the right one.

The curves calculated at 100 and 200 GeV/c practically do not differ from the one at 360 GeV/c. This is in agreement with experimental data which show that the scaling in the reaction Ia takes place already at the energy $\sim$ 10 GeV.

The proton spectra from Δ^{++}-isobar for the reaction Ia at 100, 200 and 360 GeV/c [3] are presented in Fig. 3. The theoretical curve corresponds to momentum 360 GeV/c.

In Fig. 4a the cross section $d\sigma/dM_x^2$ as a function of M_x^2 for the reaction Id at 22.4 GeV/c [6] is shown. $d\sigma/d(M_x^2/S)$ versus M_x^2/S for the reaction Ia at 100, 200 and 360 GeV/c [3] is given in Fig. 4b, and the double differential cross section $d\sigma/dt\,d(M_x^2/S)$ plotted as a function of M_x^2/S in the interval $0.1 \leq |t| \leq 0.2(\text{GeV/c})^2$, as well as in some other intervals of t is shown in Fig. 4c (see for notation the text to Fig. 2f). At low initial energy the theoretical distributions on x and M_x^2 display the structure which is related to the resonance region of the πq-scattering total cross section in the lower block of the diagram 1[1)] ($\bar{\Delta}^{--}$ in $\pi^- p^-$-scattering in Fig. 2a

1) Resonance peaks are more significant in Δ-isobar spectra than in nucleon ones [7]. This is accounted by the presence of the factor t in nucleon spectra as compared with the smooth function of t (3) in Δ-isobar spectra.

at $x = 0.98$ and at $M_x^2 \approx 1.5$ GeV^2 in Fig. 4a, as well as ρ ($x = 0.98$) and f ($x = 0.96$) in the total cross section $\pi^+\pi^-$ in Fig. 2b). At higher energies the resonance region tends to $x = 1$, and its contribution has a non-scaling form decreasing as $1/s^2$ (due to π -meson exchange). The accurate experiments in the region of small M_x^2 are of special interest.

Thus model OPER with parameters (5) describes well the behaviour of spectra in x and M_x^2 and their energy dependence.

b) Dependence on transfer momentum

The dependence on transfer momentum shows the peripheral nature of Δ -isobar formation mechanism. In Fig. 5a the cross section $d\sigma/dt'(t' = t_{min} - t)$ for the reaction Id at 22.4 GeV/c in the range $t' < 0.74$(GeV/c)^2 [6] is presented, and in Fig. 5b - for the reaction Ib at 32 GeV/c [5] . The cross section $d\sigma/dt'$ versus t' for the reactions Ia,b,c at 147 GeV/c [4] is given in Fig. 5c-e. In Fig. 5f the model predictions are compared with the experimental data on cross section $d\sigma/dt'$ for the reaction Ia at 100, 200 and 360 GeV/c [3] .

OPER predictions for the cross section $d\sigma/dt$ are compared with the experimental data on the reaction Id at 22.4 GeV/c [6] in Fig. 6a; with the data on the reaction Ib at 32 GeV/c [5] in Fig. 6b and with the data on the reaction Ia [3] in Fig. 6c.

In Fig. 7 the cross section $d\sigma/dp_\perp^2$ for the reactions Ia-c is plotted. In Fig. 7a the model predictions are compared with the data on the reaction Ib at 32 GeV/c [5], in Fig. 7b -

with the data on the reaction Id at 22.4 GeV/c [6]. In Fig.7c-f the data are given for the reaction Ia at 100, 200 and 360 GeV/c [3]. All theoretical curves in Figs 2-7 have been calculated in kinematic limits corresponding to the experimental conditions (see the explanation to Fig. 2).

4. Extraction of $\pi^{\circ}N$, $\pi\pi$, $K\pi$ and $\gamma\pi$ -total cross sections

Since the experimental data on Δ -isobar inclusive production in nucleon fragmentation region are well described by the diagram 1, this allows one to obtain, on the basis of the formula (1) the total cross section of $\pi^{\circ}N$ and $\pi\pi$ -interactions which are inaccessible for direct measuring. On doing so one is to limit himself to the region of small $|t|$ where the model predictions weakly depend on the off-mass-shell formfactor. This imposes limitations on x (large x) and $P_{\perp}$ (small $P_{\perp}$). In this region kinematic variables t, x and $P_{\perp}$ are connected by a simple relation

$$t = -\frac{P_{\perp}^2}{x} - (1-x)\left(\frac{m_{\Delta}^2}{x} - m^2\right) \qquad (7)$$

The formula (7) shows that if one chooses the value $0.05(\mathrm{GeV}/c)^2$ for the upper limit of $|t|$ then the region x and $P_{\perp}$ is limited by the following values

$$0{,}93 \leq x < 1\,; \quad P_{\perp} \leq 0{,}2 \ \mathrm{GeV}/c \qquad (8)$$

On the other hand, the estimation of background mechanisms

contribution to Δ -isobar production is also of great interest. In the model OPER such a mechanism is connected with the diagram 8a. We shall estimate the contribution of this diagram to the reaction Ia in the region (8) using the well-known contribution of the diagram 8b [7], which is the analogy of the diagram 8a in nucleon charge-exchange spectra. The ratio of the cross sections corresponding to the diagrams 8a,b is determined by the ratio of the differential cross-section sum

$$R = \frac{\frac{d\sigma}{dt}^{\pi^+p\to\pi^0\Delta^{++}}(S_2) + \frac{d\sigma}{dt}^{\pi^0p\to\pi^-\Delta^{++}}(S_2)}{\frac{d\sigma}{dt}^{\pi^-p\to\pi^0n}(S_2) + \frac{d\sigma}{dt}^{\pi^0p\to\pi^+n}(S_2)} \qquad (9)$$

Large masses of the upper block $S_2 > 4$ GeV^2 correspond to the region $x > 0.95$ (i.e. Regge-behaviour region determined by ρ -pole). In this region the ratio

$$R = 3/2 \qquad (10)$$

predicted from the sum rules for the reggeon-particle scattering amplitudes is fulfilled well [8].

In Fig. 9 the solid curve shows the contribution of the diagram 1 for the reaction Ia at $P_{lab} = 360$ GeV/c and $P_1 = 0$. The dashed curve corresponds to the contribution of the diagram 8b, multiplied by 3/2. As is seen, at $x > 0.95$ the contribution of the diagram 8a is less than 6% as compared with that of the diagram 1, therefore namely in this region the extraction of data on $\pi\pi$ -scattering seems to be most correct.

The analysis carried out can be applied also to the isobar inclusive production reactions in nucleon fragmentation

region in NN, KN and γN -collisions from which total cross sections of $\pi^{\circ}N$, $K\pi$ and $\gamma^{3}\pi$ processes may be extracted.

The authors express their thanks to K.G.Boreskov, A.B. Kaidalov and A.V.Turbiner for useful discussions.

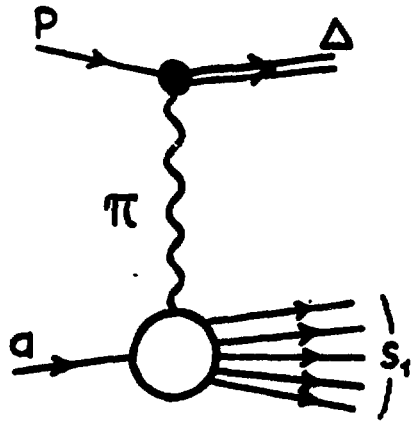

Fig. 1

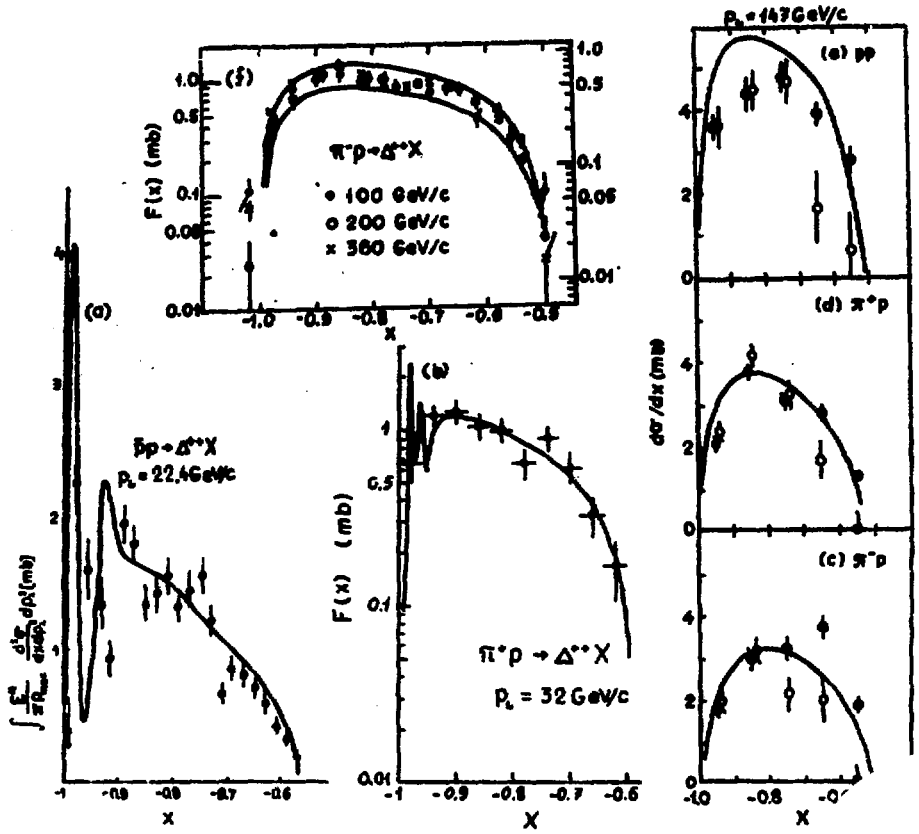
(f)
F(x) (mb)
π⁻p→Δ⁺⁺X
• 100 GeV/c
o 200 GeV/c
x 360 GeV/c
X
(a)
pp→Δ⁺⁺X
p_L = 22.4GeV/c
(b)
F(x) (mb)
π⁺p → Δ⁺⁺X
p_L = 32 GeV/c
X
p_L = 147GeV/c
(e) pp
(d) π⁺p
(c) π⁻p
dσ/dx (mb)
X

Fig. 2

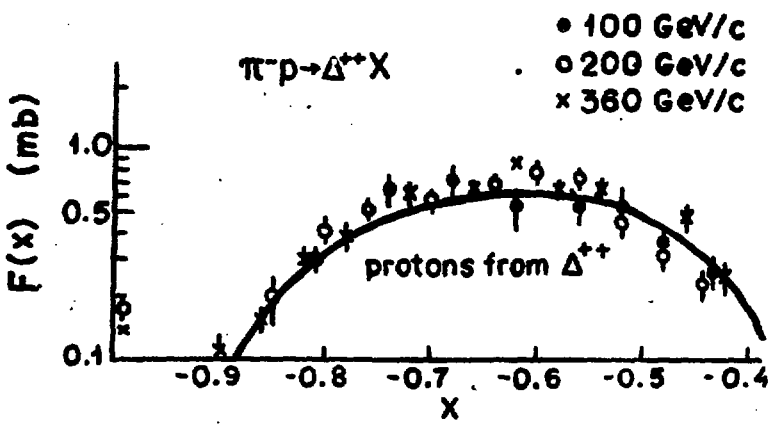
• 100 GeV/c
o 200 GeV/c
× 360 GeV/c
π⁻p→Δ⁺⁺X
F(x) (mb)
1.0
0.5
0.1
protons from Δ⁺⁺
-0.9
-0.8
-0.7
-0.6
-0.5
-0.4
X

Fig. 3

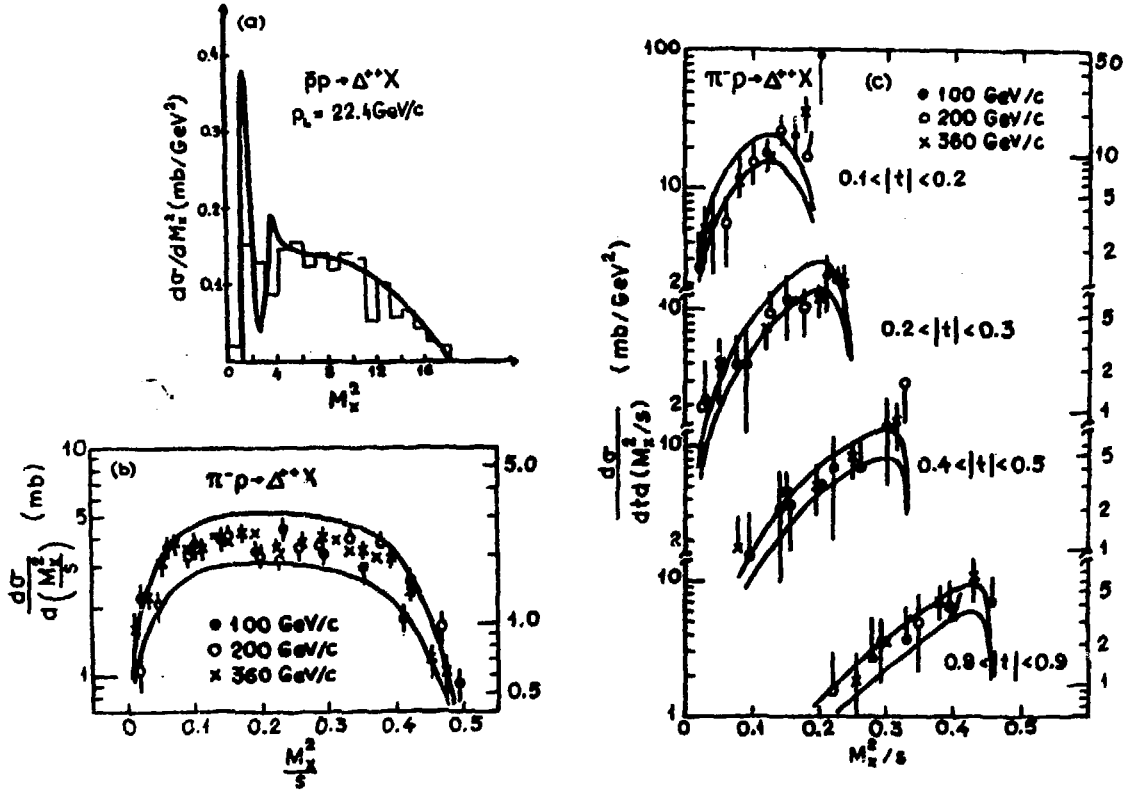
(a)
$\bar{p}p \to \Delta^{++}X$
p_L = 22.4GeV/c
$d\sigma/dM_x^2$ (mb/GeV^2)
M_x^2
(b)
$\pi^- p \to \Delta^{++}X$
$\frac{d\sigma}{d\left(\frac{M_x^2}{s}\right)}$ (mb)
• 100 GeV/c
o 200 GeV/c
× 360 GeV/c
$\frac{M_x^2}{s}$
(c)
$\pi^- p \to \Delta^{++}X$
• 100 GeV/c
o 200 GeV/c
× 360 GeV/c
0.1<|t|<0.2
0.2<|t|<0.3
0.4<|t|<0.5
0.8<|t|<0.9
$\frac{d\sigma}{dt\,d(M_x^2/s)}$ (mb/GeV^2)
M_x^2/s

Fig. 4

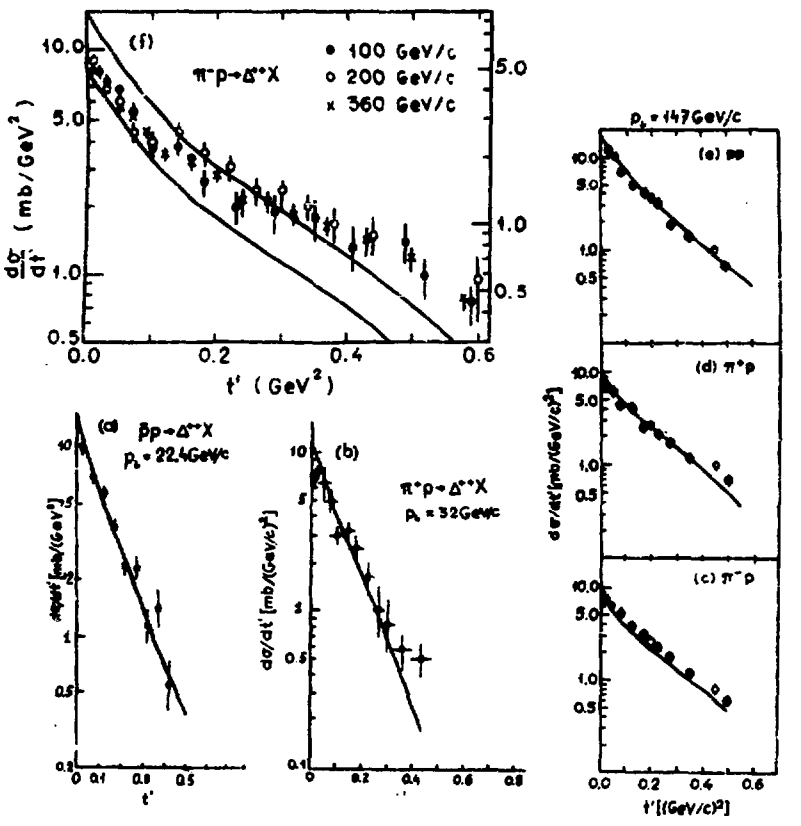
(f)
π⁻p→Δ⁰X
• 100 GeV/c
○ 200 GeV/c
× 360 GeV/c
dσ/dt' (mb/GeV²)
t' (GeV²)
(a) pp
p_L = 22.4GeV/c
(b)
π⁺p→Δ⁺⁺X
p_L = 32GeV/c
dσ/dt' [mb/(GeV/c)²]
t'
p_L = 147GeV/c
(e) pp
(d) π⁺p
(c) π⁻p
dσ/dt' [mb/(GeV/c)²]
t' [(GeV/c)²]

Fig. 5

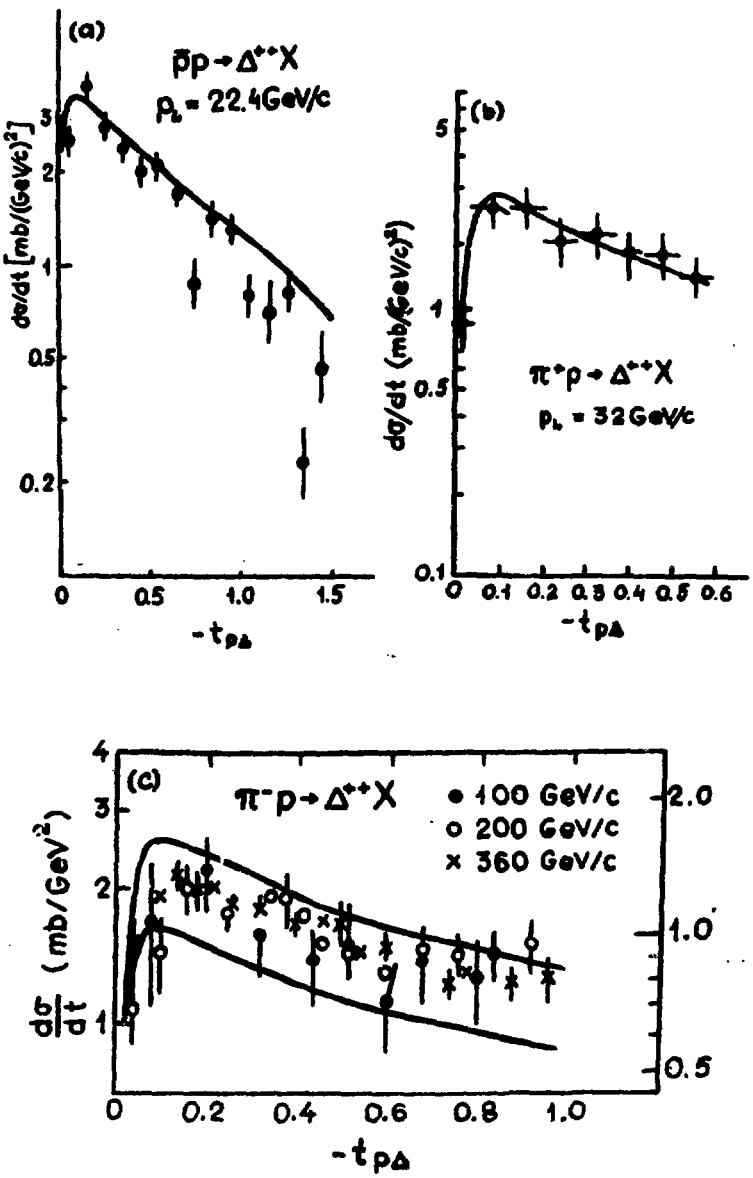
(a)
$\bar{p}p \to \Delta^{++}X$
$p_L = 22.4$GeV/c
$d\sigma/dt$ [mb/(GeV/c)^2]
$-t_{p\Delta}$
(b)
$d\sigma/dt$ (mb/(GeV/c)^2)
$\pi^+p \to \Delta^{++}X$
$p_L = 32$GeV/c
$-t_{p\Delta}$
(c)
$\pi^-p \to \Delta^{++}X$
• 100 GeV/c
o 200 GeV/c
× 360 GeV/c
$\frac{d\sigma}{dt}$ (mb/GeV^2)
$-t_{p\Delta}$

Fig. 6

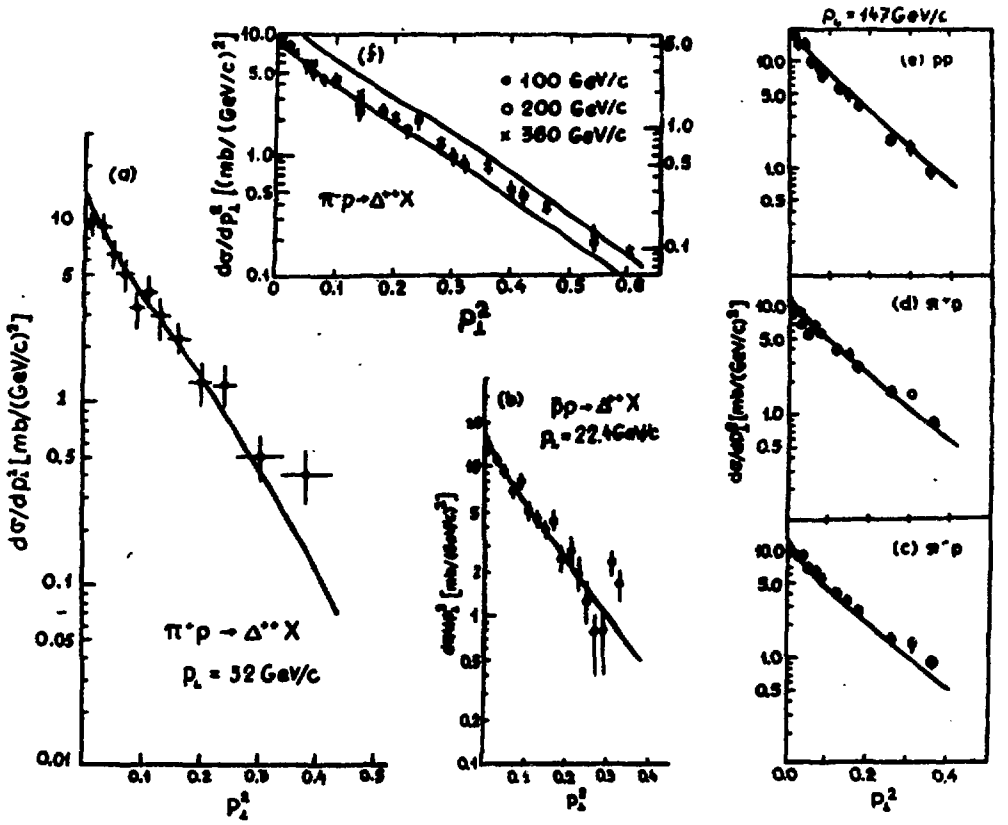
(a)
$\pi^+ p \to \Delta^{++} X$
p_L = 32 GeV/c
$d\sigma/dp_\perp^2$ [mb/(GeV/c)^2]
$p_\perp^2$
(b)
$pp \to \Delta^{++} X$
p_L = 22.4 GeV/c
(c)
(d)
(e) pp
p_L = 147 GeV/c

Fig. 7

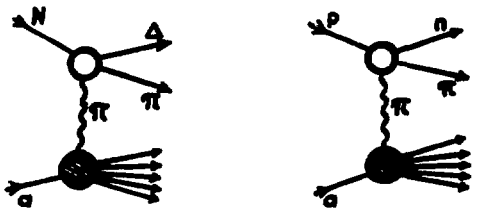

Fig. 8

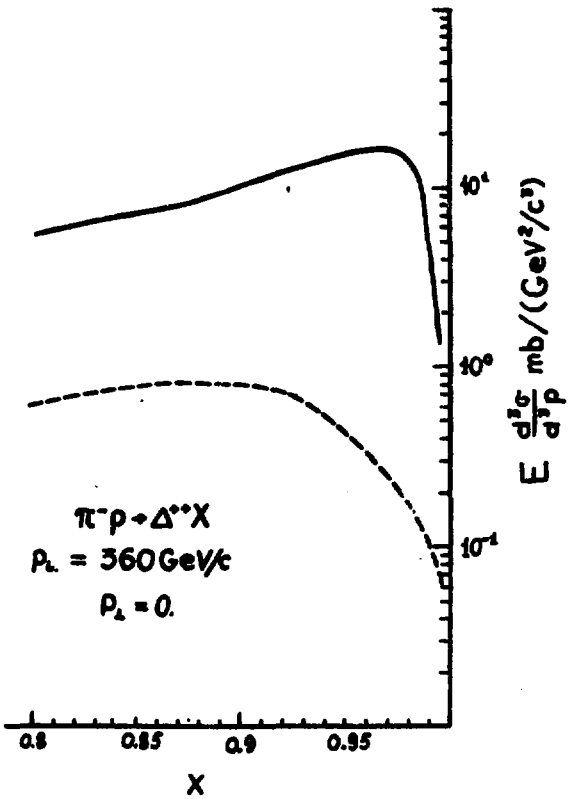
$\pi^- p \to \Delta^{++} X$
$p_L = 360\,GeV/c$
$p_\perp = 0.$
10^1
10^0
10^{-1}
0.8
0.85
0.9
0.95
X
$E\frac{d^3\sigma}{d^3p}$ mb/(GeV²/c³)

Fig. 9

Figure Captions

Fig. 1 One-pion exchange diagram for Δ -isobar spectra in ap -collisions in proton fragmentation region.

Fig. 2 Δ^{++} -isobar spectrum dependence on scaling variable x (for explanations see the text).

Fig. 3 Proton spectrum from Δ^{++}-isobar for the reaction Ia (see the text).

Fig. 4 a. $d\sigma/dM_x^2$ cross section as a function of M_x^2 for the reaction Id.

b. $d\sigma/(dM_x^2/s)$ cross section versus M_x^2/s .

c. Double differential cross section $d\sigma/dt\, d(M_x^2/s)$ dependence on M_x^2/s at fixed values of t for the reaction Ia (for explanations see the text).

Fig. 5 Comparison of theoretical calculations and experimental data on cross section $d\sigma/dt'$ for the reactions Ia-d (see the text).

Fig. 6 Distribution $d\sigma/dt$ for the reactions Ia-d (see the text).

Fig. 7 Distribution $d\sigma/dp_t^2$ for the reactions Ia-d (see the text).

Fig. 8 a. Two-block diagram for Δ -isobar spectra in aN collisions.

b. Two-block diagram for nucleon charge-exchange spectra in ap -collisions.

Fig. 9 The x -dependence of Δ^{++}-isobar spectra in the reac-

tion $\pi^- p \to \Delta^{++} X$ at $P_{lab} = 360$ GeV/c and $P_\perp = 0$. The solid curve is the contribution of the diagram 1, the dashed one - the contribution of the diagram 8a (see the text).

References

1 K.G.Boreskov, A.B.Kaidalov, L.A.Ponomarev, Proceeding of the XVII International Conference on High-Energy Physics, London, 1974

2 K.G.Boreskov, A.A.Grigoryan, A.B.Kaidalov, I.I.Levintov, Yad. Fiz. 27, 813, 1978

3 P.D.Higgins et al., Phys. Rev., D19, 731, 1979

4 D.Brick et al., Phys. Rev., D21, 632, 1980

5 I.V.Azhinenko et al., Yad. Fiz., 31, 956, 1980

6 E.G.Boos et al., Nucl. Phys., B151, 193, 1979

7 K.G.Boreskov, A.A.Grigoryan, A.B.Kaidalov, Yad. Fiz., 24, 789, 1976

8 A.A.Grigoryan, A.B.Kaidalov, Yad. Fiz., 30, 1636, 1979.

The manuscript was received 15 January 1981

Г.Г.АРАКЕЛЯН, А.А.ГРИГОРЯН

ИНКЛЮЗИВНЫЕ СПЕКТРЫ Δ^{++}-ИЗОБАР В АДРОН-АДРОННЫХ СТОЛКНОВЕНИЯХ

(на английском языке)

Ереванский физический институт

Тех.редактор А.С.Абрамян

Заказ 128 БΦ-04846 Тираж 299

Препринт ЕФИ Формат издания 60x84/16

Подписано к печати 18/III-81г. 1.5 уч.изд.л. Ц. 10 к.

Издано Отделом научно-технической информации
Ереванского физического института, Ереван-36, пер.Маркаряна 2

индекс 3624